JOURNAL OF GUIDANCE, CONTROL, AND DYNAMICS
Vol. 21, No. 5, September–October 1998

Stability and Control of a Structurally Nonlinear Aeroelastic System

Jeonghwan Ko* and Thomas W. Strganac†
Texas A&M University, College Station, Texas 77843-3141
and
Andrew J. Kurdila‡
University of Florida, Gainesville, Florida 32611-6250

The authors examine the stability properties of a class of nonlinear controls derived via feedback linearization techniques for a structurally nonlinear prototypical two-dimensional wing section. In the case in which the wing section has a single trailing-edge control surface, the stability of partial feedback linearization to achieve plunge primary control is studied. It is shown for this case that the zero dynamics associated with the closed-loop system response are locally asymptotically stable for a range of flow speeds and elastic axis locations. However, there exist locations of the elastic axis and speeds of the subsonic/incompressible flow for which this simple feedback strategy exhibits a wide range of bifurcation phenomena. Both Hopf and pitchfork bifurcations evolve parametrically in terms of the flow speed and elastic axis location. In the case in which the wing section has two control surfaces, the global stability of adaptive control techniques derived from full feedback linearization is studied. In comparison with partial or full feedback linearization techniques, the adaptive control strategies presented do not require explicit knowledge of the form of the structural nonlinearity.

Nomenclature

a	= nondimensionalized distance from the midchord to the elastic axis
b	= semichord of the wing
c_h	= structural damping coefficient in plunge due to viscous damping
c_{l_α}, c_{m_α}	= lift and moment coefficients per angle of attack
c_{l_β}, c_{m_β}	= lift and moment coefficients per control surface deflection
c_α	= structural damping coefficient in pitch due to viscous damping
h	= plunge displacement
I_α	= mass moment of inertia of the wing about the elastic axis
k_h	= structural spring constant in plunge
k_α	= structural spring constant in pitch
L	= aerodynamic lift
M	= aerodynamic moment
m	= mass
U	= freestream velocity
x_α	= nondimensionalized distance measured from the elastic axis to the center of mass
α	= pitch angle
β, β_1, β_2	= flap deflection
ρ	= density of air

I. Introduction

ALTHOUGH the underlying physics of aeroelastic phenomena have been studied for decades, some researchers in the past few years have placed particular emphasis on the role of nonlinearity in aeroelastic instabilities. For the most part, these studies have focused on the qualitative nonlinear behavior of open-loop (or uncontrolled) aeroelastic systems. Notable examples of research that are representative of this class include the work of Tang and Dowell[1] and Conner et al.,[2] who examine freeplay nonlinearities in prototypical sections, and the study of nonlinear panel flutter models by Dowell.[3] Some research does examine adaptive control of nonlinear flutter models, as in Refs. 4 and 5. Still, it is clear that there currently is a lack of knowledge of stability analyses for the closed-loop dynamics of nonlinear aeroelastic systems. This paper continues the discussion of the approach described in Ref. 6, wherein partial and full feedback linearization of a simple class of nonlinear aeroelastic systems is studied. In contrast to Ref. 6, where the focus was to employ Lie algebraic methods to derive feedback controllers, this paper studies the parametric stability and bifurcation structure of the resulting closed-loop dynamical systems. One primary conclusion of this paper is that plunge primary control, derived via partial feedback linearization techniques, exhibits a wide range of bifurcation phenomena for different flow regimes and elastic axis locations. A second conclusion of the paper is that adaptive control methods based on full feedback linearization techniques exhibit global stability.

II. Equations of Motion

Following the strategy employed in Ref. 6, we seek to employ the most simple representation of the aeroelastic system as possible, while retaining sufficient terms to account for the well-documented nonlinear response observed in low-speed wind-tunnel experiments.[7] Hence, the governing equations of motion for the aeroelastic system under consideration (see Fig. 1) are taken as

$$\begin{bmatrix} m & mx_\alpha b \\ mx_\alpha b & I_\alpha \end{bmatrix} \begin{Bmatrix} \ddot{h} \\ \ddot{\alpha} \end{Bmatrix} + \begin{bmatrix} c_h & 0 \\ 0 & c_\alpha \end{bmatrix} \begin{Bmatrix} \dot{h} \\ \dot{\alpha} \end{Bmatrix} + \begin{bmatrix} k_h & 0 \\ 0 & k_\alpha(\alpha) \end{bmatrix} \begin{Bmatrix} h \\ \alpha \end{Bmatrix} = \begin{Bmatrix} -L \\ M \end{Bmatrix} \tag{1}$$

The location of the elastic axis may be varied in the experimental structure we are modeling. The term $k_\alpha(\alpha)$ is the nonlinear spring stiffness associated with the pitching motion. In this paper, as a

Presented as Paper 97-1024 at the AIAA/ASME/ASCE/AHS/ASC 38th Structures, Structural Dynamics, and Materials Conference, Kissimmee, FL, April 7–10, 1997; received Oct. 3, 1997; revision received April 6, 1998; accepted for publication April 7, 1998.

*Postdoctoral Research Associate, Department of Aerospace Engineering. Member AIAA.
†Associate Professor, Department of Aerospace Engineering. Associate Fellow AIAA.
‡Associate Professor, Department of Aerospace Engineering, Mechanics, and Engineering Science. Member AIAA.

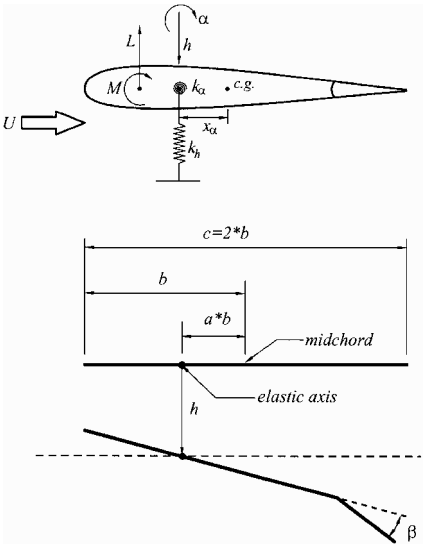

Fig. 1 Aeroelastic model.

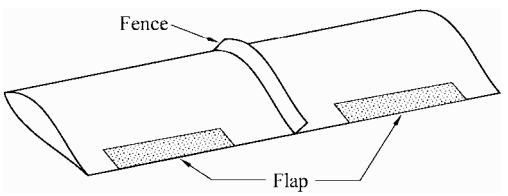

Fig. 2 Wing section with two control surfaces.

special class of nonlinear stiffness, we assume that the spring force $k_\alpha(\alpha)$ is represented by the following polynomial expression:

$$k_\alpha(\alpha) = k_{\alpha_0} + k_{\alpha_1}\alpha + k_{\alpha_2}\alpha^2 + k_{\alpha_3}\alpha^3 + k_{\alpha_4}\alpha^4 + \cdots \tag{2}$$

where the coefficients k_{α_i} are obtained from measured experimental pitch angle vs moment data. One may question the validity of the preceding polynomial representation of nonlinear stiffness because of the presence of odd-order terms. It is noted that these terms have been added to emphasize that the spring coefficients are obtained from fitting the measured data; i.e., the best fit to the experimental data may actually be nonsymmetric. In the case in which we have a single trailing-edge actuation surface, we assume that the quasisteady aerodynamic force L and moment M are modeled[8] as

$$L = \rho U^2 b c_{l_\alpha}\left[\alpha + (\dot{h}/U) + \left(\tfrac{1}{2} - a\right)b(\dot{\alpha}/U)\right] + \rho U^2 b c_{l_\beta}\beta$$
$$M = \rho U^2 b^2 c_{m_\alpha}\left[\alpha + (\dot{h}/U) + \left(\tfrac{1}{2} - a\right)b(\dot{\alpha}/U)\right] + \rho U^2 b^2 c_{m_\beta}\beta \tag{3}$$

Although the quasisteady aerodynamic model adopted in this paper is relatively simple, we emphasize that the main objective of the theoretical development in this paper is to analyze the closed-loop system characteristics via feedback linearization continuing our analysis in Ref. 6. Furthermore, the reduced frequency associated with the experiments that complement this effort validates our use of the quasisteady model.

We will also study prototypical wing sections with two control surfaces in this paper. We consider the case in which both control surfaces are located on the trailing edge as depicted in Fig. 2. For this case, we assume that the ratio of control surface separation to span is large and limit considerations to small angle of attack and control surface deflections. For two control surfaces along the trailing edge, the aerodynamic loads are represented as follows:

$$L = \rho U^2 b c_{l_\alpha}\left[\alpha + (\dot{h}/U) + \left(\tfrac{1}{2} - a\right)b(\dot{\alpha}/U)\right] + \rho U^2 b c_{l_{\beta_1}}\beta_1 + \rho U^2 b c_{l_{\beta_2}}\beta_2 \tag{4}$$

$$M = \rho U^2 b^2 c_{m_\alpha}\left[\alpha + (\dot{h}/U) + \left(\tfrac{1}{2} - a\right)b(\dot{\alpha}/U)\right] + \rho U^2 b^2 c_{m_{\beta_1}}\beta_1 + \rho U^2 b^2 c_{m_{\beta_2}}\beta_2 \tag{5}$$

With substitution of the aerodynamic loads into the equations of motion, we obtain

$$\begin{bmatrix} m & mx_\alpha b \\ mx_\alpha b & I_\alpha \end{bmatrix}\begin{Bmatrix} \ddot{h} \\ \ddot{\alpha} \end{Bmatrix} + \begin{bmatrix} c_h + \rho U b c_{l_\alpha} & \rho U b^2 c_{l_\alpha}\left(\frac{1}{2} - a\right) \\ \rho U b^2 c_{m_\alpha} & c_\alpha - \rho U b^3 c_{m_\alpha}\left(\frac{1}{2} - a\right) \end{bmatrix}\begin{Bmatrix} \dot{h} \\ \dot{\alpha} \end{Bmatrix} + \begin{bmatrix} k_h & \rho U^2 b c_{l_\alpha} \\ 0 & -\rho U^2 b^2 c_{m_\alpha} + k_\alpha(\alpha) \end{bmatrix}\begin{Bmatrix} h \\ \alpha \end{Bmatrix} = \begin{bmatrix} -\rho b c_{l_{\beta_1}} & -\rho b c_{l_{\beta_2}} \\ \rho b^2 c_{m_{\beta_1}} & \rho b^2 c_{m_{\beta_2}} \end{bmatrix}\begin{Bmatrix} \beta_1 \\ \beta_2 \end{Bmatrix} U^2 \tag{6}$$

It is important to note that the sole source of nonlinearity in these equations arises from the polynomial nonlinearity $k_\alpha(\alpha)$. In addition, Eqs. (6) are nearly identical in form to the equations of motion for a wing section with leading-edge and trailing-edge control surfaces (see Ref. 9). Thus, the stability analysis that follows applies to the leading-/trailing-edge configuration with little modification.

III. Stability Analysis of Plunge Primary Control

Among the numerous methodologies for the control of nonlinear systems,[10] it has been shown in Ref. 6 that partial feedback linearization techniques[10,11] may be employed for the case of a single trailing-edge control surface. If the nonlinear partial feedback linearization is constructed so as to explicitly control the pitch degree of freedom, the zero dynamics of the closed-loop system are linear as shown in Ref. 6. In this case, a fairly complete understanding of the stability regions for the controller as a function of elastic axis location a and flow speed U may be derived. On the other hand, if a nonlinear partial feedback linearization technique is employed to explicitly control the plunge degree of freedom, the question of closed-loop stability is considerably more difficult.

For the subsequent derivation, it is necessary to express the equations of motion [Eqs. (1–3)] in a state-space form

$$\dot{\boldsymbol{x}} = \boldsymbol{f}_\mu(\boldsymbol{x}) + \boldsymbol{g}_\mu(\boldsymbol{x})\beta \tag{7}$$

where the state variables are defined as

$$\boldsymbol{x} \equiv \begin{Bmatrix} x_1 \\ x_2 \\ x_3 \\ x_4 \end{Bmatrix} \triangleq \begin{Bmatrix} h \\ \alpha \\ \dot{h} \\ \dot{\alpha} \end{Bmatrix} \tag{8}$$

and

$$\boldsymbol{f}_\mu = \begin{Bmatrix} x_3 \\ x_4 \\ -k_1 x_1 - \left[k_2 U^2 + p(x_2)\right]x_2 - c_1 x_3 - c_2 x_4 \\ -k_3 x_1 - \left[k_4 U^2 + q(x_2)\right]x_2 - c_3 x_3 - c_4 x_4 \end{Bmatrix}$$
$$\boldsymbol{g}_\mu = \begin{Bmatrix} 0 \\ 0 \\ g_3 \\ g_4 \end{Bmatrix} U^2 \tag{9}$$

For the sake of brevity, a set of new variables is introduced and tabulated in Table 1.

The plunge primary control derived in Ref. 6 is achieved by introducing the change of variables $\boldsymbol{\Phi} \equiv T(\boldsymbol{x})$

$$\boldsymbol{\Phi} \equiv \begin{Bmatrix} \phi_1 \\ \phi_2 \\ \phi_3 \\ \phi_4 \end{Bmatrix} \triangleq \begin{Bmatrix} x_1 \\ x_3 \\ x_2 \\ g_3 x_4 - g_4 x_3 \end{Bmatrix} \tag{10}$$

Table 1 System variables

$$d = m\left(I_\alpha - mx_\alpha^2 b^2\right)$$
$$k_1 = I_\alpha k_h / d$$
$$k_2 = \left(I_\alpha \rho b c_{l_\alpha} + mx_\alpha b^3 \rho c_{m_\alpha}\right)\Big/ d$$
$$k_3 = -mx_\alpha b k_h / d$$
$$k_4 = \left(-mx_\alpha b^2 \rho c_{l_\alpha} - m\rho b^2 c_{m_\alpha}\right)\Big/ d$$
$$p(x_2) = (-mx_\alpha b/d)k_\alpha(x_2)$$
$$q(x_2) = (m/d)k_\alpha(x_2)$$
$$c_1 = \left[I_\alpha\left(c_h + \rho U b c_{l_\alpha}\right) + mx_\alpha \rho U b^3 c_{m_\alpha}\right]\Big/ d$$
$$c_2 = \left[I_\alpha \rho U b^2 c_{l_\alpha}\left(\tfrac{1}{2} - a\right) - mx_\alpha b c_\alpha + mx_\alpha \rho U b^4 c_{m_\alpha}\left(\tfrac{1}{2} - a\right)\right]\Big/ d$$
$$c_3 = \left(-mx_\alpha b c_h - mx_\alpha \rho U b^2 c_{l_\alpha} - m\rho U b^2 c_{m_\alpha}\right)\Big/ d$$
$$c_4 = \left[mc_\alpha - mx_\alpha \rho U b^3 c_{l_\alpha}\left(\tfrac{1}{2} - a\right) - m\rho U b^3 c_{m_\alpha}\left(\tfrac{1}{2} - a\right)\right]\Big/ d$$
$$g_3 = \left(-I_\alpha \rho b c_{l_\beta} - mx_\alpha b^3 \rho c_{m_\beta}\right)\Big/ d$$
$$g_4 = \left(mx_\alpha b^2 \rho c_{l_\beta} + m\rho b^2 c_{m_\beta}\right)\Big/ d$$

which is linear. We should emphasize that the preceding transformation is based on the objective to control the plunge motion and is obtained through a standard procedure for partial feedback linearization as shown in Ref. 6. The transformed governing equations of motion for the case of a single trailing-edge actuator may be written as

Table 2 System parameters

Parameter	Value
b, m	0.135
m, kg	12.3870
I_α, kg · m^2	0.065
r_{cg}	$0.0873 - (b + a \cdot b)$
x_α	r_{cg}/b
ρ, kg/m^3	1.225
span, m	0.6
c_{l_α}	6.28
k_h, N/m	2844.4
c_{l_β}	3.358
c_h, Ns/m	27.43
c_{m_α}	$(0.5 + a)c_{l_\alpha}$
c_{m_β}	−0.635
$k_\alpha(\alpha)$	see Eq. (47)

It now should be clear that ϕ_1 and ϕ_2 can be regulated by any linear control methodology. As stated in Ref. 6, however, a sufficient condition for the local asymptotic stability of the closed-loop system is that the internal or zero dynamics space (obtained by setting $\phi_1 = \phi_2 = 0$) is asymptotically stable. The equations that must be studied in this case may be written as

$$\begin{Bmatrix} \dot{\phi}_3 \\ \dot{\phi}_4 \end{Bmatrix} = \begin{Bmatrix} A_{34}\phi_4 \\ [g_4 Q_U(\phi_3) - g_3 P_U(\phi_3)]\phi_3 + A_{44}\phi_4 \end{Bmatrix} \tag{16}$$

$$\begin{Bmatrix} \dot{\phi}_1 \\ \dot{\phi}_2 \\ \dot{\phi}_3 \\ \dot{\phi}_4 \end{Bmatrix} = \begin{pmatrix} \phi_1 \\ -k_1\phi_1 - [c_1 + c_2(g_4/g_3)]\phi_2 - Q_U(\phi_3)\phi_3 - (c_2/g_3)\phi_4 \\ (g_4/g_3)\phi_2 + (1/g_3)\phi_4 \\ \begin{Bmatrix} (g_4k_1 - g_3k_3)\phi_1 + \left[c_1 g_4 + c_2\left(g_4^2/g_3\right) - c_3 g_3 - c_4 g_4\right]\phi_2 \\ +[g_4 Q_U(\phi_3) - g_3 P_U(\phi_3)]\phi_3 + [c_2(g_4/g_3) - c_4]\phi_4 \end{Bmatrix} \end{pmatrix} + \begin{Bmatrix} 0 \\ g_3 \\ 0 \\ 0 \end{Bmatrix} U^2\beta \tag{11}$$

where

$$P_U(\phi_3) = k_4 U^2 + q(\phi_3), \qquad Q_U(\phi_3) = k_2 U^2 + p(\phi_3) \tag{12}$$

These equations may be written succinctly as

$$\dot{\boldsymbol{\Phi}} = \boldsymbol{F}_{\boldsymbol{\mu}}(\boldsymbol{\Phi}) + \boldsymbol{G}_{\boldsymbol{\mu}}(\boldsymbol{\Phi})\beta \tag{13}$$

where the subscript $\boldsymbol{\mu}$ represents a vector of parameters $\boldsymbol{\mu} = (a, U)$. In other words, the open-loop (and closed-loop) dynamics depend parametrically on elastic axis location a and flow velocity U. From elementary considerations in Lie algebraic control methods (see Ref. 11), we select the nonlinear partially linearizing feedback control to be

$$\beta = \frac{k_1\phi_1 + [c_1 + c_2(g_4/g_3)]\phi_2 + Q_U(\phi_3)\phi_3 + (c_2/g_3)\phi_4 + v}{U^2 g_3} \tag{14}$$

where v is a new, yet to be determined, control input. The resulting closed-loop equations are then

$$\dot{\phi}_1 = \phi_2, \qquad \dot{\phi}_2 = v, \qquad \dot{\phi}_3 = A_{32}\phi_2 + A_{34}\phi_4$$
$$\dot{\phi}_4 = A_{41}\phi_1 + A_{42}\phi_2 + [g_4 Q_U(\phi_3) - g_3 P_U(\phi_3)]\phi_3 + A_{44}\phi_4 \tag{15}$$

where

$$A_{32} = g_4/g_3, \qquad A_{34} = 1/g_3, \qquad A_{41} = g_4k_1 - g_3k_3$$
$$A_{42} = c_1 g_4 + c_2\left(g_4^2/g_3\right) - c_3 g_3 - c_4 g_4$$
$$A_{44} = c_2(g_4/g_3) - c_4$$

To gain an appreciation for the difficulty in assessing the stability of Eq. (16), we must recall that the coefficients A_{34}, $Q_U(\phi_3)$, $P_U(\phi_3)$, and A_{44} depend parametrically on elastic axis location a and flow velocity U. By expanding these coefficients as explicit functions of the physical system parameters a and U, we can express Eq. (16) as a nonlinear second-order oscillator equation

$$\ddot{w} + B_0(a, U)\dot{w} + B_1(a, U)w + B_2(a, U)w^2 + B_3(a, U)w^3 + \cdots = 0 \tag{17}$$

where

$$w = \phi_3$$
$$B_0(a, U) = -\frac{\rho U b^3\left(c_{l_\alpha}c_{l_\beta}a^3 - c_{l_\alpha}c_{m_\beta}a - \frac{1}{4}c_{l_\alpha}c_{l_\beta}\right) + \frac{1}{2}c_{l_\alpha}c_{m_\beta}}{-I_\alpha c_{l_\beta} - 0.0873mbc_{m_\beta} + mb^2c_{m_\beta} + mb^2c_{m_\beta}a}$$
$$B_1(a, U) = \frac{\rho U^2 b^2\left(c_{l_\alpha}c_{l_\beta}a + \frac{1}{2}c_{l_\alpha}c_{l_\beta} - c_{l_\alpha}c_{m_\beta}\right) - c_{l_\beta}k_{\alpha_0}}{-I_\alpha c_{l_\beta} - 0.0873mbc_{m_\beta} + mb^2c_{m_\beta} + mb^2c_{m_\beta}a}$$
$$B_2(a, U) = \frac{-c_{l_\beta}k_{\alpha_1}}{-I_\alpha c_{l_\beta} - 0.0873mbc_{m_\beta} + mb^2c_{m_\beta} + mb^2c_{m_\beta}a}$$
$$B_3(a, U) = \frac{-c_{l_\beta}k_{\alpha_2}}{-I_\alpha c_{l_\beta} - 0.0873mbc_{m_\beta} + mb^2c_{m_\beta} + mb^2c_{m_\beta}a}$$
$$\vdots \tag{18}$$

In the preceding equations, the number 0.0873 arises from substituting x_α (see Table 2). Equation (17) suggests that the parametric

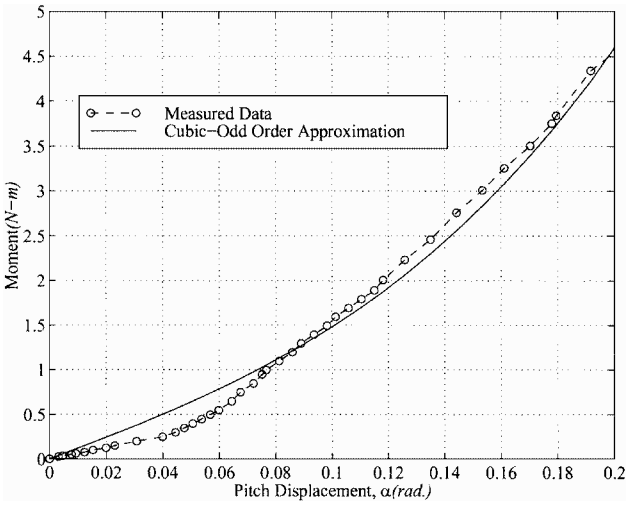

Fig. 3 Cubic odd-order polynomial approximation of the nonlinear spring.

dependence of the equations governing the zero dynamics will yield a rich bifurcation structure. For example, we observe that Eq. (17) represents a family of ordinary differential equations that includes well-known special cases such as Duffing's equation

$$\ddot{x} + h\dot{x} - (1 - x^2)(x/2) = D\cos \nu t \tag{19}$$

which has been used to motivate discussions of aeroelastic flutter in Ref. 12.

To simplify our analysis of the second-order oscillator in Eq. (17), we assume that the polynomial nonlinearity $k_\alpha(\alpha)$ has the form

$$k_\alpha(\alpha) = k_{\alpha_0} + k_{\alpha_2}\alpha^2$$

or, equivalently, the nonlinear torsional stiffness has the form

$$\alpha k_\alpha(\alpha) = \left(k_{\alpha_0} + k_{\alpha_2}\alpha^2\right)\alpha$$

Although higher-order and quadratic terms have been studied by several researchers,[7,13–15] Fig. 3 shows that this choice yields a reasonable representation of the spring stiffness. By inspection of Eq. (17), the preceding assumption implies that

$$B_2(a, U) = B_4(a, U) = B_5(a, U) = 0$$

so that the equations governing the zero dynamics may be written as

$$\begin{Bmatrix} \dot{w} \\ \ddot{w} \end{Bmatrix} = \begin{bmatrix} 0 & 1 \\ -B_1(a, U) & -B_0(a, U) \end{bmatrix} \begin{Bmatrix} w \\ \dot{w} \end{Bmatrix} + \begin{Bmatrix} 0 \\ -B_3(a, U)w^3 \end{Bmatrix} \left(\triangleq \boldsymbol{f}_w\right) \tag{20}$$

or as

$$\ddot{w} + B_0(a, U)\dot{w} + B_1(a, U)w + B_3(a, U)w^3 = 0 \tag{21}$$

Finally, if we are free to vary B_0, B_1, and B_3 independently, the study of the stability would reduce to a form considered by several authors (see Ref. 16 or the classical examples in Ref. 17). The functions $B_0(a, U)$, $B_1(a, U)$, and $B_3(a, U)$ are clearly dependent as depicted in Eq. (18). For the derivations to follow, the contour plots of B_0, B_1, and B_3 are shown in Fig. 4. The parameter values that are used for these calculations are tabulated in Table 2.

For the cubic oscillator [Eq. (20)], it is well known that, depending on the coefficient functions B_0, B_1, and B_3 or the parameters a and U, there exist either one or three equilibrium points. When $B_1/B_3 < 0$, there exist three fixed points, including the origin:

$$(w, \dot{w}) = \begin{cases} (0, 0) \\ \left(+\sqrt{-(B_1/B_3)}, 0\right) \\ \left(-\sqrt{-(B_1/B_3)}, 0\right) \end{cases}$$

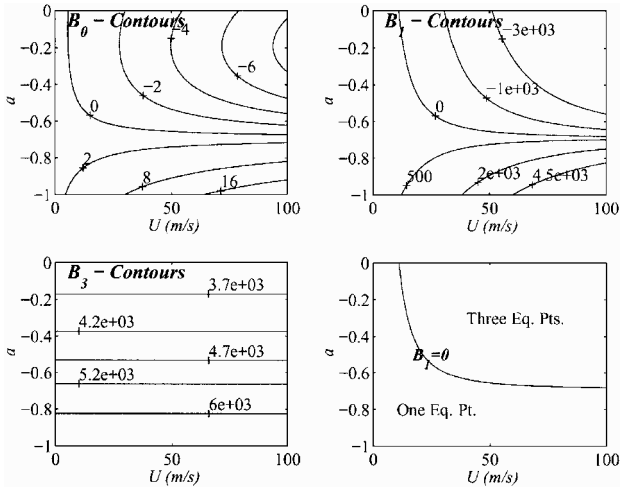

Fig. 4 Contour plots of the functions, $B_0(a, U)$, $B_1(a, U)$, and $B_2(a, U)$.

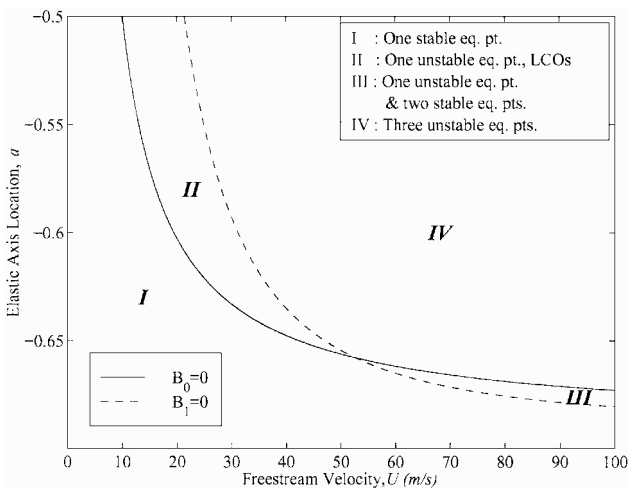

Fig. 5 Regions with different stability characteristics.

To address the local stability of each equilibrium point, the Jacobian matrices evaluated at each of the equilibrium points are obtained as

$$\left[\frac{\partial \boldsymbol{f}_w}{\partial \boldsymbol{w}}\right] = \begin{bmatrix} 0 & 1 \\ \left(-B_1 - 3B_3 w^2\right) & -B_0 \end{bmatrix} \tag{22}$$

$$\left[\frac{\partial \boldsymbol{f}_w}{\partial \boldsymbol{w}}\right]_{(0,0)} = \begin{bmatrix} 0 & 1 \\ -B_1 & -B_0 \end{bmatrix} \tag{23}$$

$$\left[\frac{\partial \boldsymbol{f}_w}{\partial \boldsymbol{w}}\right]_{\left(\pm\sqrt{-(B_1/B_3)}, 0\right)} = \begin{bmatrix} 0 & 1 \\ 2B_1 & -B_0 \end{bmatrix} \tag{24}$$

Next, we will investigate the stability characteristics of this oscillator in the two parameter space—(a, U).

A. One-Fixed-Point Case

For the wind-tunnel experiment at Texas A&M University, we have utilized

$$c_{l_\beta} = 3.358, \qquad k_{\alpha_0} = 12.1382, \qquad k_{\alpha_2} = 269.4149$$

Furthermore, it is easy to check that the denominator of B_3 is a function of the elastic axis location a and is negative for all $a \in [-1, 0]$.

Because $B_3 > 0$ for the range of parameters under consideration (see Fig. 4), when $B_1 > 0$, there is only one equilibrium point [the origin $(0, 0)$]. Thus, as shown in Fig. 4, the contour line $B_1 = 0$ divides the parameter space into two separate regions: one with only one equilibrium point and the other with three equilibrium points.

The stability of the single equilibrium point $(0, 0)$ [found below the dashed line representing $B_1(a, U) = 0$ in Fig. 5] may be

analyzed by investigating the eigenvalues of the Jacobian matrix in Eq. (23). The characteristic equation for the Jacobian matrix is

$$\lambda^2 + B_0\lambda + B_1 = 0$$

Because we have $B_1 > 0$, we conclude that, if $B_0 > 0$, then both eigenvalues are stable. If $B_0 < 0$, the eigenvalues are unstable. The parameter region where both B_0 and B_1 are positive is marked as I and is shown in Fig. 5. In region II, the single equilibrium point is unstable because $B_0 < 0$ and $B_1 > 0$.

B. Three-Fixed-Point Case

When $B_1 < 0$, there exist two other equilibrium points in addition to the origin. First, for the origin, the eigenvalues of the Jacobian matrix [Eq. (23)] are

$$\lambda = \frac{-B_0 \pm \sqrt{B_0 - 4B_1}}{2}$$

It is not difficult to observe that because $B_1 < 0$ and $|B_1| \gg |B_0|$ from Fig. 4, the origin has negative and positive eigenvalues; i.e., it is a saddle point.

For the two new fixed points, $\{\pm\sqrt{[-(B_1/B_3)]}, 0\}$, the characteristic equation of the Jacobian matrix in Eq. (24) is

$$\lambda^2 + B_0\lambda - 2B_1 = 0$$

We immediately note that, if $B_0 > 0$, the two fixed points are stable, and if $B_0 < 0$, the fixed points are unstable. In Fig. 5, the region IV is where $B_0 < 0$, and the two fixed points are unstable in that region. The function satisfies $B_0 > 0$ in the region III, and thus the two new equilibrium points are stable. When the two new fixed points are stable, the trajectory of the system is attracted to either one of the two points, depending on the initial conditions. The stable and unstable manifolds for this case may be found in Ref. 6, and analogous results for Duffing's equation have been examined by others (for example, see Ref. 18).

C. Center Manifold Analysis

It is well known in nonlinear dynamics that when the Jacobian matrix of a fixed point has nonhyperbolic or zero eigenvalues, careful analysis is required to analyze the local stability of the fixed point. In our current derivation, it is obvious that when $B_1 = 0$, the Jacobian will have a zero eigenvalue. A standard methodology to analyze a system of this characteristic is to use center manifold analysis.[19,20]

Consider a path in parameter space along the contour connecting P and Q in Fig. 6. Along this path we have

$$B_1(a, U) \equiv 0$$

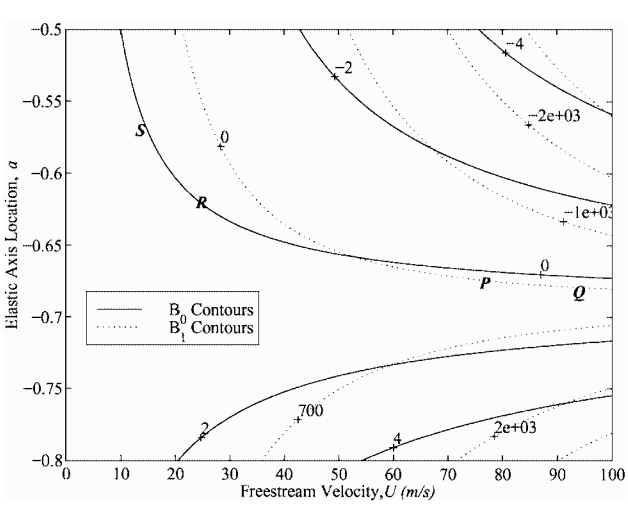

Fig. 6 Paths on the segment B_0 and $B_1 = 0$: ——, B_0 contours, and · · · · ·, B_1 contours.

and Eq. (20) becomes

$$\begin{Bmatrix} \dot{w} \\ \ddot{w} \end{Bmatrix} = \begin{bmatrix} 0 & 1 \\ 0 & -B_0(a, U) \end{bmatrix} \begin{Bmatrix} w \\ \dot{w} \end{Bmatrix} + \begin{Bmatrix} 0 \\ -B_3(a, U)w^3 \end{Bmatrix} \tag{25}$$

The eigenvalues of the linear part are given by $\lambda_1 = 0$ and $\lambda_2 = -B_0(a, U)$. By noting that the generalized eigenvectors of the linear part of the preceding matrix are

$$[\Psi] = \left[\begin{Bmatrix} 1 \\ 0 \end{Bmatrix} \begin{Bmatrix} -1 \\ B_0 \end{Bmatrix} \right]$$

we can transform the governing equations into the form

$$\begin{Bmatrix} \dot{\eta}_1 \\ \dot{\eta}_2 \end{Bmatrix} = \begin{bmatrix} 0 & 0 \\ 0 & -B_0 \end{bmatrix} \begin{Bmatrix} \eta_1 \\ \eta_2 \end{Bmatrix} \begin{Bmatrix} -(B_3/B_0)(\eta_1 - \eta_2)^3 \\ -(B_3/B_0)(\eta_1 - \eta_2)^3 \end{Bmatrix} \tag{26}$$

Note that we have introduced the change of variables

$$\begin{Bmatrix} w \\ \dot{w} \end{Bmatrix} = \begin{bmatrix} 1 & -1 \\ 0 & B_0 \end{bmatrix} \begin{Bmatrix} \eta_1 \\ \eta_2 \end{Bmatrix} \tag{27}$$

in Eq. (26). Thus, unless $B_0 = 0$, we may apply the center manifold theorem and may conclude that the center manifold is given by the graph of a function (at least locally) that is tangent to the center eigenspace.[19,20] That is, we seek to find a manifold of the form

$$W^C = \{(\eta_1, \eta_2) : \eta_2 = h(\eta_1)\} \tag{28}$$

But this fact implies that we can write

$$\dot{\eta}_1 = -(B_3/B_0)[\eta_1 - h(\eta_1)]^3 \tag{29}$$

from the first partition of Eq. (26). Likewise, the second partition of Eq. (26) yields

$$\dot{\eta}_2 = h'(\eta_1)\dot{\eta}_1 = -B_0 h(\eta_1) - (B_3/B_0)[\eta_1 - h(\eta_1)]^3 \tag{30}$$

If we make the power series expansion

$$h(\eta_1) \triangleq c_2\eta_1^2 + c_3\eta_1^3 + \mathcal{O}\left(\eta_1^4\right) \tag{31}$$

we find that

$$\begin{aligned} &-\left[2c_2\eta_1 + 3c_3\eta_1^2 + \mathcal{O}\left(\eta_1^3\right)\right](B_3/B_0)\left[\eta_1 - c_2\eta_1^2 - c_3\eta_1^3 + \mathcal{O}\left(\eta_1^4\right)\right]^3 \\ &\quad = -B_0\left[c_2\eta_1^2 + c_3\eta_1^3 + \mathcal{O}\left(\eta_1^4\right)\right] \\ &\quad\quad - (B_3/B_0)\left[\eta_1 - c_2\eta_1^2 - c_3\eta_1^3 + \mathcal{O}\left(\eta_1^4\right)\right]^3 \end{aligned} \tag{32}$$

Equating like powers of η_1 implies that

$$c_2 = 0, \qquad c_3 = -\left(B_3 \big/ B_0^2\right)$$

The graph of the center manifold is approximately given by

$$\eta_2 = -\left(B_3 \big/ B_0^2\right)\eta_1^3 \tag{33}$$

The equations of motion along the center manifold may be approximated by substituting Eq. (33) into Eq. (29):

$$\dot{\eta}_1 = -(B_3/B_0)\eta_1^3 \tag{34}$$

Because $B_0 > 0$ and $B_1 > 0$ along the path from P to Q, we conclude that the local dynamics are stable.

D. Hopf Bifurcation

Another interesting case occurs when $B_0 = 0$. Consider the path in parameter space along the contour from R to S in Fig. 6. Along this path

$$B_0(a, U) = 0$$

so that

$$\begin{Bmatrix} \dot{w} \\ \ddot{w} \end{Bmatrix} = \begin{bmatrix} 0 & 1 \\ -B_1 & 0 \end{bmatrix} \begin{Bmatrix} w \\ \dot{w} \end{Bmatrix} + \begin{Bmatrix} 0 \\ -B_3(a, U)w^3 \end{Bmatrix} \tag{35}$$

The eigenvalues for the linear part of Eq. (35) are $\lambda = \pm\sqrt{(-B_1)}$ and are purely imaginary because $B_1 > 0$.

By introducing the change of variables

$$\begin{Bmatrix} \eta_1 \\ \eta_2 \end{Bmatrix} = \begin{bmatrix} \sqrt{B_1} & 0 \\ 0 & 1 \end{bmatrix} \begin{Bmatrix} w \\ \dot{w} \end{Bmatrix}$$

we obtain the normal form of the governing equations

$$\begin{Bmatrix} \dot{\eta}_1 \\ \dot{\eta}_2 \end{Bmatrix} = \begin{bmatrix} 0 & \sqrt{B_1} \\ -\sqrt{B_1} & 0 \end{bmatrix} \begin{Bmatrix} \eta_1 \\ \eta_2 \end{Bmatrix} + \begin{Bmatrix} 0 \\ -\left(B_3 \big/ B_1^{\frac{3}{2}}\right)\eta_1^3 \end{Bmatrix} \tag{36}$$

Because the Jacobian matrix has nonhyperbolic eigenvalues, the higher-order term $-(B_3/B_1^{3/2})\eta_1^3$ will determine the stability of the system.[20] Because we have $B_3 > 0$, and $B_1 > 0$ on the path $R-S$, we conclude that the trajectories are bounded as η_1 grows.

IV. Adaptive Control with Two Control Surfaces

It has been shown in Ref. 6 that for the case when we have two separate control surfaces, as shown in Fig. 2, full feedback linearization may be achieved provided that

$$c_{l_{\beta_1}} c_{m_{\beta_2}} - c_{m_{\beta_1}} c_{l_{\beta_2}} \neq 0 \tag{37}$$

In other words, the invertibility of the control influence matrix $[B]$ guarantees that we may transform the nonlinear equation into an equivalent linear system and obtain a globally stable closed-loop system using any reasonable linear control design method. Based on the results in Ref. 6, an adaptive control method may be derived for the case when we do not exactly know the expansion coefficients for the nonlinear stiffness in pitch.

For simplicity, we rewrite Eq. (6) symbolically as

$$[M]\ddot{\boldsymbol{x}} + ([C_0] + [C_U])\dot{\boldsymbol{x}} + ([K_0] + [K_U])\boldsymbol{x} + [W(\boldsymbol{x})]\boldsymbol{q} = U^2[B]\boldsymbol{\beta} \tag{38}$$

where

$$\boldsymbol{x} = \begin{Bmatrix} h \\ \alpha \end{Bmatrix}, \qquad [K_0] = \begin{bmatrix} k_h & 0 \\ 0 & 0 \end{bmatrix}$$

$$[K_U] = \begin{bmatrix} 0 & \rho U^2 b c_{l_\alpha} \\ 0 & -\rho U^2 b^2 c_{m_\alpha} \end{bmatrix}, \qquad [C_0] = \begin{bmatrix} c_h & 0 \\ 0 & c_\alpha \end{bmatrix}$$

$$[C_U] = \begin{bmatrix} \rho U b c_{l_\alpha} & \rho U b^2 c_{l_\alpha}\left(\frac{1}{2} - a\right) \\ \rho U b^2 c_{m_\alpha} & -\rho U b^3 c_{m_\alpha}\left(\frac{1}{2} - a\right) \end{bmatrix}$$

$$\boldsymbol{q} = [k_{\alpha_0} \quad k_{\alpha_1} \quad k_{\alpha_2} \quad k_{\alpha_3} \quad k_{\alpha_4}]^T, \qquad \boldsymbol{\beta} = \begin{Bmatrix} \beta_1 \\ \beta_2 \end{Bmatrix}$$

$$[W(\boldsymbol{x})] = \begin{Bmatrix} (0 & 0 & 0 & 0 & 0) \\ (\alpha & \alpha^2 & \alpha^3 & \alpha^4 & \alpha^5) \end{Bmatrix}$$

The reader should note that the nonlinear stiffness terms associated with the pitch angle α have been isolated in the term $[W(\boldsymbol{x})]\boldsymbol{q}$. Also, the stiffness and damping terms are divided into constant terms and terms dependent on the flow velocity.

We assume that the coefficients $\boldsymbol{q}$ of the polynomial nonlinearity are unknown. We may derive an adaptive controller for this system that is stable, where estimates $\hat{\boldsymbol{q}}(t)$ of $\boldsymbol{q}(t)$ evolve simultaneously with solution of the governing equations (38). Because we derive a control law based on the Lyapunov stability theory,[10,21] let us assume the following form of the Lyapunov function:

$$V = \tfrac{1}{2}\dot{\boldsymbol{x}}^T[M]\dot{\boldsymbol{x}} + \tfrac{1}{2}\boldsymbol{x}^T\{[K_a] + [K_0]\}\boldsymbol{x} + \tfrac{1}{2}\boldsymbol{e}^T[\Lambda]^{-1}\boldsymbol{e} \tag{39}$$

where $[K_a]$ and $[\Lambda]$ are arbitrary positive definite matrices, and the estimation error has been defined as $\boldsymbol{e} = \boldsymbol{q} - \hat{\boldsymbol{q}}$. Clearly, V is positive definite. The derivative of this Lyapunov function along the system trajectory is obtained as

$$\dot{V} = \dot{\boldsymbol{x}}^T\Big\{-([C_0] + [C_U])\dot{\boldsymbol{x}} - ([K_0] + [K_U])\boldsymbol{x} - [W(\boldsymbol{x})]\boldsymbol{q} + U^2[B]\boldsymbol{\beta}\Big\} + \dot{\boldsymbol{x}}^T\Big\{[K_a] + [K_0]\Big\}\boldsymbol{x} + \dot{\boldsymbol{e}}^T[\Lambda]^{-1}\boldsymbol{e} \tag{40}$$

The standard strategy for obtaining a stabilizing controller based on the Lyapunov function is to choose a control input from the derivative of the Lyapunov function that makes the derivative negative definite. From Eq. (40), a possible candidate for the control is

$$\boldsymbol{\beta}(t) = (1/U^2)[B]^{-1}\{[W(\boldsymbol{x})]\hat{\boldsymbol{q}} + ([K_U] - [K_a])\boldsymbol{x} + ([C_U] - [C_a])\dot{\boldsymbol{x}}\} \tag{41}$$

with the positive definite matrix $[C_a]$ introduced to add damping to the system. The preceding feedback control law utilizes the estimate $\hat{\boldsymbol{q}}$ and is based on the assumption that the control influence matrix is invertible; i.e., Eq. (37) is satisfied. With this control input $\boldsymbol{\beta}$, $\dot{V}$ becomes

$$\dot{V} = \dot{\boldsymbol{x}}^T\{-([C_0] + [C_a])\dot{\boldsymbol{x}} - [W(\boldsymbol{x})]\boldsymbol{e}\} + \dot{\boldsymbol{e}}^T[\Lambda]^{-1}\boldsymbol{e} \tag{42}$$

Because we obtain the derivative of the estimation error as $\dot{\boldsymbol{e}} = -\dot{\hat{\boldsymbol{q}}}$, let us assume that the estimate of the unknown parameters $\hat{\boldsymbol{q}}$ evolve according to the following equation:

$$\dot{\hat{\boldsymbol{q}}}(t) = -[\Lambda]^T[W(\boldsymbol{x})]^T\dot{\boldsymbol{x}} \tag{43}$$

After Eq. (43) is substituted into Eq. (42), the derivative of the Lyapunov function becomes

$$\dot{V} = -\dot{\boldsymbol{x}}^T\{[C_0] + [C_a]\}\dot{\boldsymbol{x}} \tag{44}$$

We conclude that $\dot{V}$ is negative semidefinite because it does not have any terms dependent on $\boldsymbol{x}$ and $\boldsymbol{q}$. Although the semidefiniteness generally does not guarantee the asymptotic convergence of trajectories to the equilibrium points, we may use the invariant set theorem by La Salle and Lefschetz,[21] to prove that the closed-loop system is attracted to a small set.

Theorem 1. Suppose we choose the feedback control law

$$\boldsymbol{\beta}(t) = \frac{1}{U^2}[B]^{-1}\left\{[W(\boldsymbol{x})]\hat{\boldsymbol{q}} + \begin{bmatrix} 0 & \rho U^2 b c_{l_\alpha} \\ 0 & -\rho U^2 b^2 c_{m_\alpha} \end{bmatrix}\boldsymbol{x} + \begin{bmatrix} \rho U b c_{l_\alpha} & \rho U b^2 c_{l_\alpha}\left(\frac{1}{2} - a\right) \\ \rho U b^2 c_{m_\alpha} & -\rho U b^3 c_{m_\alpha}\left(\frac{1}{2} - a\right) \end{bmatrix}\dot{\boldsymbol{x}} - [C_a]\dot{\boldsymbol{x}} - [K_a]\boldsymbol{x}\right\}$$

and the identification update law

$$\dot{\hat{\boldsymbol{q}}}(t) = -[\Lambda]^T[W(\boldsymbol{x})]^T\dot{\boldsymbol{x}} \tag{45}$$

where $[C_a]$, $[K_a]$, and $[\Lambda]$ are arbitrary symmetric positive definite matrices. Then, the trajectories $\boldsymbol{x}(t)$, $\dot{\boldsymbol{x}}(t)$, and $\hat{\boldsymbol{q}}(t)$ are attracted to the largest positive invariant subset of

$$\mathcal{M} \triangleq \{(\boldsymbol{x}, \dot{\boldsymbol{x}}, \hat{\boldsymbol{q}}) : \dot{V}(\boldsymbol{x}, \dot{\boldsymbol{x}}, \hat{\boldsymbol{q}}) = 0\} \tag{46}$$

where

$$V(\boldsymbol{x}, \dot{\boldsymbol{x}}, \hat{\boldsymbol{q}}) \equiv \frac{1}{2}\dot{\boldsymbol{x}}^T[M]\dot{\boldsymbol{x}} + \frac{1}{2}\boldsymbol{x}^T\left\{[K_a] + \begin{bmatrix} k_h & 0 \\ 0 & 0 \end{bmatrix}\right\}\boldsymbol{x} + \frac{1}{2}(\boldsymbol{q} - \hat{\boldsymbol{q}})^T[\Lambda]^{-1}(\boldsymbol{q} - \hat{\boldsymbol{q}})$$

Proof. The preceding theorem is a direct application of the invariant manifold theorem.[10,21] □

By using Theorem 1, we conclude that the system trajectories converge to the equilibrium point of the system. However, we do not necessarily have the convergence of the estimation of the unknown parameters to the real values.

To validate this derived adaptive control methodology, numerical experiments are performed based on the experimental model of Texas A&M University.[14,15,22] The physical parameters used in these numerical simulations are tabulated in Table 2. The nonlinear stiffness term $k_\alpha(\alpha)$ is obtained by fitting the measured displacement-moment data as a fourth-order polynomial[14]

$$k_\alpha(\alpha) = 2.82(1 - 22.1\alpha + 1315.5\alpha^2 - 8580\alpha^3 + 17289.7\alpha^4) \tag{47}$$

For the initial conditions, $h = 0.01$ m and $\alpha = 0.1$ rad, flow velocity $U = 20$ m/s, and the uncontrolled response of the aeroelastic system is shown in Fig. 7 for elastic axis location, $a = -0.6$. Clearly the response exhibits limit cycle oscillations as noted by several authors.[6,7,13] With the controller derived in this section, the closed-loop system response is shown in Fig. 8. The following matrices are used in deriving the controller,

$$[K_a] = [I_2], \qquad [\Lambda] = [I_5], \qquad [C_a] = 0.03 \times [I_2]$$

where $[I_n]$ implies a $n \times n$ identity matrix. Observe that the response converges to the origin very quickly despite the fact that the initial conditions of the unknown stiffness coefficients are chosen as

$$\hat{\boldsymbol{q}}(t=0) = [1 \quad 1 \quad 1 \quad 1 \quad 1]^T$$

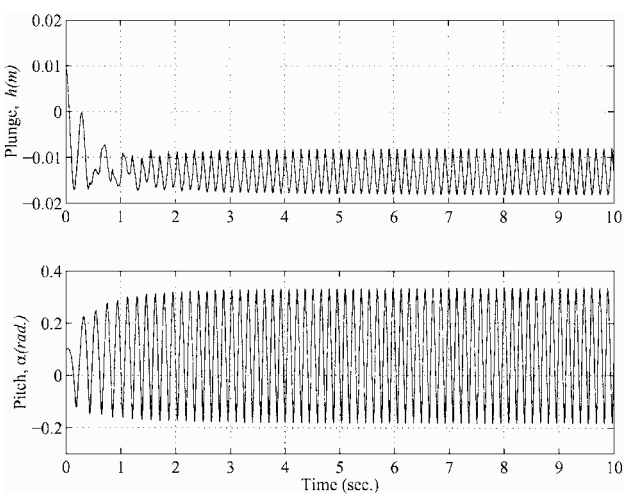

Fig. 7 Time response for open-loop system.

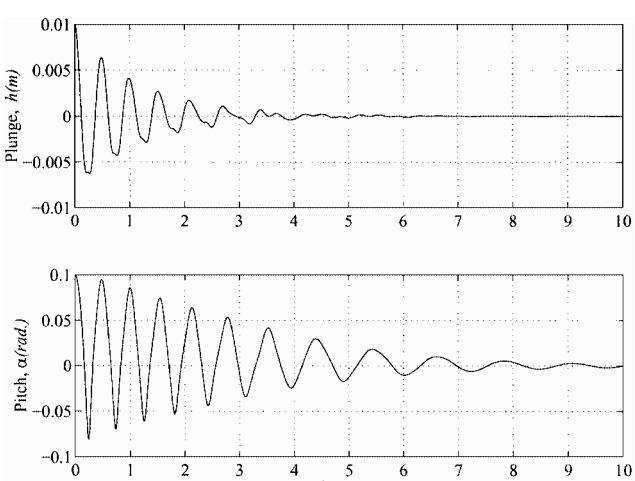

Fig. 8 Time response for closed-loop system.

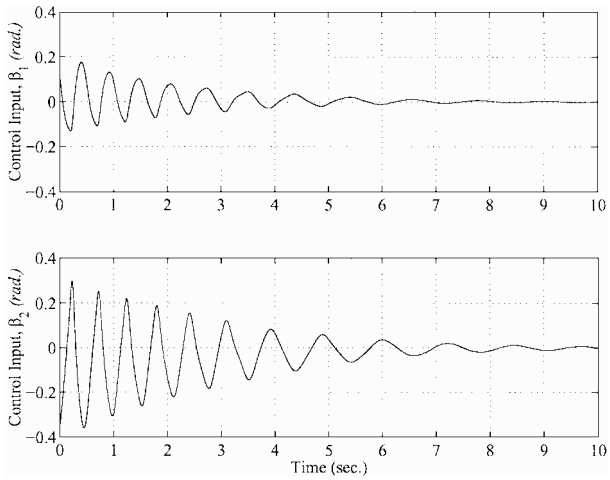

Fig. 9 Control input history.

The corresponding history of control inputs are shown in Fig. 9. For brevity, the response of the parameter estimation is not shown. However, it should be emphasized that the preceding derived adaptive law does not require the convergence of the parameters to exact values. Careful inspection of the results in Figs. 8 and 9 illustrate that although the stability guarantees in Theorem 1 are reassuring, they still leave many issues unresolved. For example, in Fig. 9 we see that the second control surface must deflect through 0.6 rad in $\frac{1}{4}$ s to affect the control in this validation study. Obviously, saturation would result in real scenarios. Thus, although the derived control methods stabilize a class of polynomial nonlinear plants, other common sources of nonlinearity, including saturation and hysteresis, are not addressed. These topics should be addressed in further research.

V. Conclusion

The authors have shown that a class of nonlinear feedback control methods derived from partial feedback linearization techniques are locally asymptotically stable for some flow regimes and elastic axis locations. However, a wide variety of bifurcation structures, including Andropov–Hopf bifurcations, are evident in the closed-loop system dynamics for some choices of flow speed and elastic axis locations. For systems having two control surfaces, it is also shown that stable adaptive control methods may be derived. The stability analysis in this case relies on a semidefinitive Lyapunov function. The class of adaptive methods is attractive in that they do not require explicit knowledge of the structure of the inherent pitch-axis nonlinearity.

References

[1] Tang, D. M., and Dowell, E. H., "Flutter and Stall Response of a Helicopter Blade with Structural Nonlinearity," *Journal of Aircraft*, Vol. 29, No. 5, 1992, pp. 953–960.

[2] Conner, M. D., Tang, D. M., Dowell, E. H., and Virgin, L. N., "Nonlinear Behavior of a Typical Airfoil Section with Control Surface Freeplay: A Numerical and Experimental Study," *Journal of Fluids and Structures*, Vol. 11, No. 1, 1997, pp. 89–109.

[3] Dowell, E. H., *Aeroelasticity of Plates and Shells*, Noordhoff International, Leyden, The Netherlands, 1975, pp. 38–43.

[4] Pak, C., Friedmann, P. P., and Livne, E., "Digital Adaptive Flutter Suppression and Simulations Using Approximate Transonic Dynamics," *Journal of Vibration and Control*, Vol. 1, No. 4, 1995, pp. 363–388.

[5] Friedmann, P. P., Guillot, D., and Presente, E., "Adaptive Control of Aeroelastic Instabilities in Transonic Flow and Its Scaling," *Journal of Guidance, Control, and Dynamics*, Vol. 20, No. 6, 1997, pp. 1190–1199.

[6] Ko, J., Kurdila, A. J., and Strganac, T. W., "Nonlinear Control of a Prototypical Wing Section with Torsional Nonlinearity," *Journal of Guidance, Control, and Dynamics*, Vol. 20, No. 6, 1997, pp. 1181–1189.

[7] O'Neil, T., Gilliatt, H. C., and Strganac, T. W., "Investigations of Aeroelastic Response for a System with Continuous Structural Nonlinearity," AIAA Paper 96-1390, April 1996.

[8] Fung, Y. C., *An Introduction to the Theory of Aeroelasticity*, Wiley, New York, 1955, pp. 207–215.

[9] Lazarus, K., Crawley, E., and Lin, C. Y., "Fundamental Mechanisms of Aeroelastic Control with Control Surface and Strain Actuation," *Journal of Guidance, Control, and Dynamics*, Vol. 18, No. 1, 1995, pp. 10–17.

[10]Slotine, J. E., and Li, W., *Applied Nonlinear Control*, Prentice–Hall, Englewood Cliffs, NJ, 1991, pp. 207–275.

[11]Isidori, A., *Nonlinear Control Systems*, Springer–Verlag, New York, 1989, pp. 1–82.

[12]Zhao, L. C., and Yang, Z. C., "Chaotic Motions of an Airfoil with Nonlinear Stiffness in Incompressible Flow," *Journal of Sound and Vibration*, Vol. 138, No. 2, 1990, pp. 245–254.

[13]Block, J. J., and Strganac, T. W., "Applied Active Control for a Nonlinear Aeroelastic Structure," *Journal of Guidance, Control, and Dynamics* (to be published).

[14]O'Neil, T., and Strganac, T. W., "An Experimental Investigation of Nonlinear Aeroelastic Response," *Journal of Aircraft*, Vol. 35, No. 4, 1998.

[15]O'Neil, T., and Strganac, T. W., "Nonlinear Aeroelastic Response—Analyses and Experiments," AIAA Paper 96-0014, Jan. 1996.

[16]Virgin, L. N., and Erickson, B. K., "A New Approach to the Overturning Stability of Floating Structures," *Ocean Engineering*, Vol. 21, No. 1, 1994, pp. 67–80.

[17]Nayfeh, A. H., and Mook, D. T., *Nonlinear Oscillations*, Wiley, New York, 1978, pp. 75–102.

[18]Dowell, E. H., and Pezeshki, C., "On the Understanding of Chaos in Duffings Equations Including a Comparison with Experiment," *Journal of Applied Mechanics*, Vol. 53, March 1986, pp. 5–9.

[19]Guckenheimer, J., and Holmes, P., *Nonlinear Oscillations, Dynamical Systems, and Bifurcations of Vector Fields*, Springer–Verlag, New York, 1983, pp. 123–145.

[20]Wiggins, S., *Introduction to Applied Nonlinear Dynamical Systems and Chaos*, Springer–Verlag, New York, 1990, pp. 193–237.

[21]La Salle, J., and Lefschetz, S., *Stability by Liapunov's Direct Method*, Academic, New York, 1961, pp. 56–71.

[22]Ko, J., Strganac, T. W., and Kurdila, A. J., "Adaptive Feedback Linearization for the Control of a Typical Wing Section with Structural Nonlinearity," *Nonlinear Dynamics* (to be published).